SNOW EXTENT MAPPING IN ALPINE AREAS USING POLARIMETRIC SAR DATA

Audrey Martini[1], Jean-Pierre Dedieu[2], Laurent Ferro-Famil[1], Monique Bernier[3] and Eric Pottier[1]

1. IETR/CNRS, Univ. Rennes1, Bât. 11D, 263 av Gén Leclerc, CS 74205, 35042 Rennes Cedex, France; audrey.martini(at)univ-rennes1.fr
2. LGGE/CNRS, 54 rue Molière. Dom. Universitaire, BP.96, 38402 St. Martin d'Hères Cedex, France
3. INRS-Eau, Terre, Environnement, 490 rue de la Couronne, Québec (Québec), G1K 9A9, Canada

ABSTRACT

This paper proposes an original technique to map the snow extent in the French Alps from SAR measurements using SIR-C fully polarimetric winter/summer data sets at L and C-bands. The method relies on a multi-frequency two-step approach. Basic natural media types, like surface and forest, are first discriminated over the scene under observation from a polarimetric analysis of summer measurements at L-band. Secondly, the presence of snow is then detected separately over each media type using the *H-A-*$\underline{\alpha}$ polarimetric decomposition theorem. An original PCVE (polarimetric contrast variation enhancement) procedure provides optimal emission/reception polarisation states that maximise the C-band winter to summer response of snow-covered areas. The results are compared to Landsat optical images acquired simultaneously.

Keywords: Snow mapping, radar polarimetry, optimisation method.

INTRODUCTION

The localisation of dry snow in alpine environments using intermediate frequency SAR data (L and C-bands) still remains a problematic application (1). Indeed, at such frequencies, dry snow is a low attenuation medium and only slightly affects the backscattered signal amplitude. Moreover alpine areas are characterised by a wide variety of underlying media with changing characteristics and important topography that may strongly affect a scene response. Dry snow mapping is an important product for global snow monitoring, widely used in the frame of hydrological applications, like Snow Water Equivalent determination (2). This paper presents a polarimetric method to map the dry snow extent in alpine areas using multi-frequency and multi-temporal polarimetric SAR data. Due to the variability of alpine environments the method is split up into three steps. A first part is dedicated to the classification of the scene into surface and forest types from summer data sets at L-band. Each media is then processed separately. The presence of snow is detected over surfaces by means of two compared methods at C-band: a) an Optimisation of Polarimetric Contrast Enhancement (OPCE) and b) a new optimisation method, based on a Polarimetric Contrast Variation Enhancement (PCVE). Snow covered forests are analysed from summer to winter variations of polarimetric decomposition results at C-band. Merged discrimination results are finally analysed through a quantitative estimation of the detection performance.

METHODS

Test Sites and SAR data

The fully polarimetric method is applied to the SIR-C/X-SAR shuttle mission over two south French Alps test sites (44°15'N, 007°15'E) during April and October 1994. Multi-temporal fully polarimetric SAR data sets were acquired at L and C-bands in both snow free (3 October 1994) and snow (12 April 1994) conditions. A validation step of snow behaviour is provided by optical Landsat images under snow versus snow-free conditions and simultaneous ground control measurements (automatic and manual network). The test sites, Risoul (300 km^2) and Izoard (800 km^2), are composed of three main alpine environments: high altitude unvegetated surfaces, medium to high altitude

forested zones and low altitude valleys. Due to the early morning acquisition time (6h GMT), both test sites are partly covered by frozen spring snow. The snow cover altitude ranges from 1200 m up to 3000 m where its depth reaches 2 m.

Principle of snow cover discrimination

Due to the high variability of alpine natural media, a technique to map the snow extent is required to identify at first the type of underlying background, i.e. surface or forest, in order to adapt the decision process. A sequential three-step approach, based on a multi-temporal polarimetric study is proposed. Figure 1 describes a flowchart of the proposed dry snow mapping algorithm.

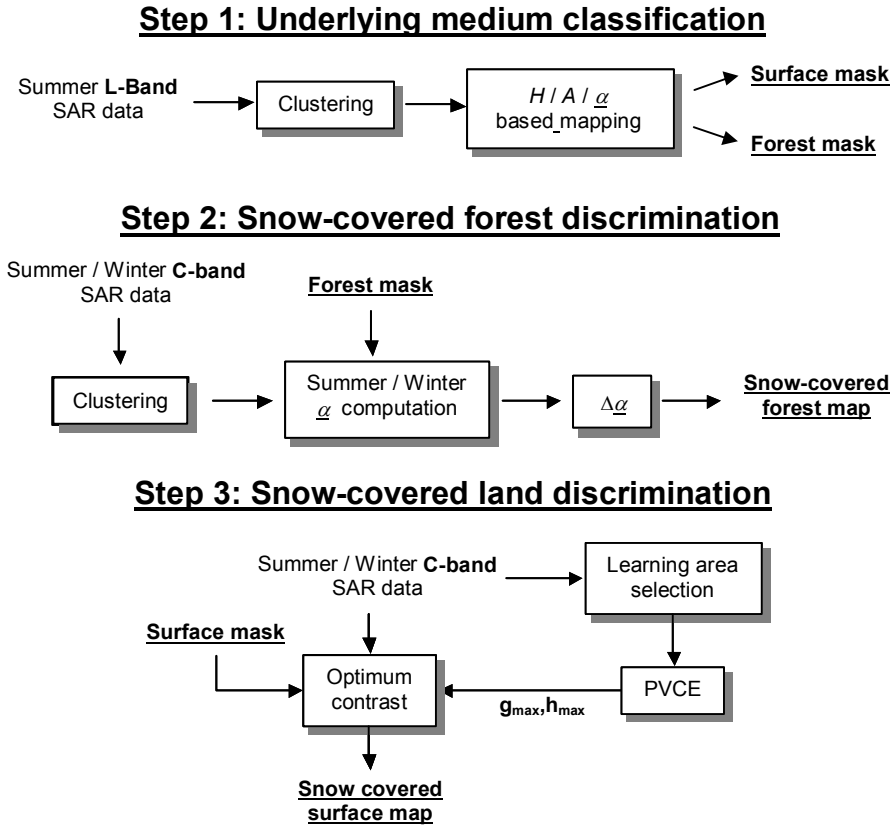

Figure 1: The three-step snow mapping algorithm.

The first step is dedicated to the discrimination of basic natural media types, like surface and forest, using a polarimetric analysis of summer measurements at L-band. The second phase of the process concerns the study of the detected surface areas. This part relies on an original Polarimetric Contrast Variation Enhancement (PCVE) procedure providing optimal emission/reception polarisation states that maximise C-band winter to summer contrast ratios over snow-covered surfaces (3). Finally, snow-covered forests are separated from snow-free ones using seasonal variations of the $\underline{\alpha}$ indicator at C-band.

Classification of the scenes

The polarimetric backscattering behaviour may be expressed in terms of a polarimetric coherency matrix, **T**. It is a (3×3) complex representation, widely used to characterise incoherent polarimetric scattering properties of natural media. It can be built from each polarimetric channel backscattering cross section, σ_{pq}, or directly from coherent scattering coefficients (4) as follows:

$$\mathbf{T} = \left\langle \mathbf{k}\mathbf{k}^{*T} \right\rangle \quad , \quad \mathbf{k} = \frac{1}{\sqrt{2}}\left[S_{hh} + S_{vv} \quad S_{hh} - S_{vv} \quad 2S_{hv}\right]^T \tag{1}$$

It has been shown that relevant parameters, H, A and $\underline{\alpha}$, can be extracted from **T** to characterise physical scattering characteristics (5). Such parameters are obtained from the projection of a dis-

tributed coherency matrix onto its eigenvector basis, as proposed by (4). This approach decomposes a coherency matrix into a weighted sum of three matrices of rank one:

$$\mathbf{T} = \mathbf{V}\mathbf{\Lambda}\mathbf{V}^{-1} = \sum_{k=1}^{3} \lambda_k \cdot \mathbf{v}_k \mathbf{v}_k^{*T} \tag{2}$$

with λ_k , the *k*th eigenvalue of **T** and $\mathbf{v}_k$ its related eigenvector.

An efficient estimation of the nature of scattering mechanisms over natural scenes can be achieved by gathering results obtained from the *H*-*A*-$\underline{\alpha}$ polarimetric decomposition and segmentation techniques. The entropy, *H*, indicates the degree of statistical disorder of the scattering phenomenon. The anisotropy, *A*, is defined as the relative importance of the secondary scattering mechanisms and the angle $\underline{\alpha}$ indicates the nature of the dominant scattering mechanism. The whole image is decomposed into segments using unsupervised statistical procedures (6). Segments are then split into independent spatial clusters over which a decision is taken. Each cluster is a group of connected pixels with a similar polarimetric behaviour.

Forest mapping

It is known that at L-band, a forest is a depolarising medium and its response is characterised by a highly random aspect. The entropy, *H*, and the anisotropy, *A*, polarimetric indicators may be used to discriminate forest from less depolarizing media. *H* and *A* are generally jointly considered to estimate the distribution of a coherency matrix eigenvalue using the following relation:

$$HA + (1-H)A + H(1-A) + (1-H)(1-A) = 1 \tag{3}$$

The four terms of Eq. (3) are positive and may be associated to different configurations of the eigenvalue set. The specific $H(1-A)$ term is equal to 0 in case of deterministic scattering and reaches 1 when the scattered wave polarisation is random. Forested areas may then be detected using the following decision rule:

$$H(1-A) > HA, (1-H)A, (1-H)(1-A) \geq H(1-A) > 0.5 \tag{4}$$

In practice *H* and *A* are estimated over a cluster and the threshold is fixed to 0.6 in order to reduce the sensitivity to perturbing factors.

Land cover mapping

Once the forested regions have been localised, a method based on the estimation of the number of relevant scattering contributions is used to detect the land covers. At L-band, in the case of a single dominant scattering mechanism, a cluster is assigned to the surface class if α_1<45°, where α_1 is the angle α of the first matrix obtained from the polarimetric decomposition (7). For two significant scattering mechanisms, the nature of the scattering mechanism is determined by comparing the first two diagonal elements of coherency matrices.

Snow-covered forest discrimination

Polarimetric analysis

Table 1 shows statistics of $\underline{\alpha}$ and *H* variations with snow conditions, computed from the SIR-C C-band data sets. In Table 1, $\langle \Delta x \rangle$ stands for the October to April average variation of *x* (equal to $\underline{\alpha}$ or *H*) and $\mathrm{std}(\Delta x)$ for its standard deviation. The temporal average variation of *x* is calculated over a reasonable number of representative clusters of the forested regions. At C-band, the polarimetric parameter $\underline{\alpha}$ may be a suitable indicator to detect the presence of snow over forested areas.

Indeed snow-covered forests show an important decrease of $\underline{\alpha}$ while snow-free forests have an almost constant polarimetric behaviour. This variation is generated by the attenuation of double bounce and volume scattering contributions by the snow layer. From the mean value and standard deviation of $\Delta\underline{\alpha}$ a decision threshold value equal to 4° is chosen. Dry snow is detected over a for-

ested area if:

$$\Delta \underline{\alpha} > 4° \quad (5)$$

Table 1: Statistics of $\underline{\alpha}$ *and* H *variations over forests.*

	Snow free		Snow	
	$\langle \Delta x \rangle$	std(Δx)	$\langle \Delta x \rangle$	std(Δx)
$x = \underline{\alpha}$	1.64	1.96	6.77	2.01
$x =$ H	0.019	0.021	0.074	0.027

Application

The $\underline{\alpha}$ variation based decision process is led, using C-band data, over the forest class. The results of the snow-covered forest discrimination are depicted in Figure 2, and a comparison with Landsat optical images in Figure 4 indicates the good performance of this polarimetric approach. The results of the performance estimation are presented in the last section.

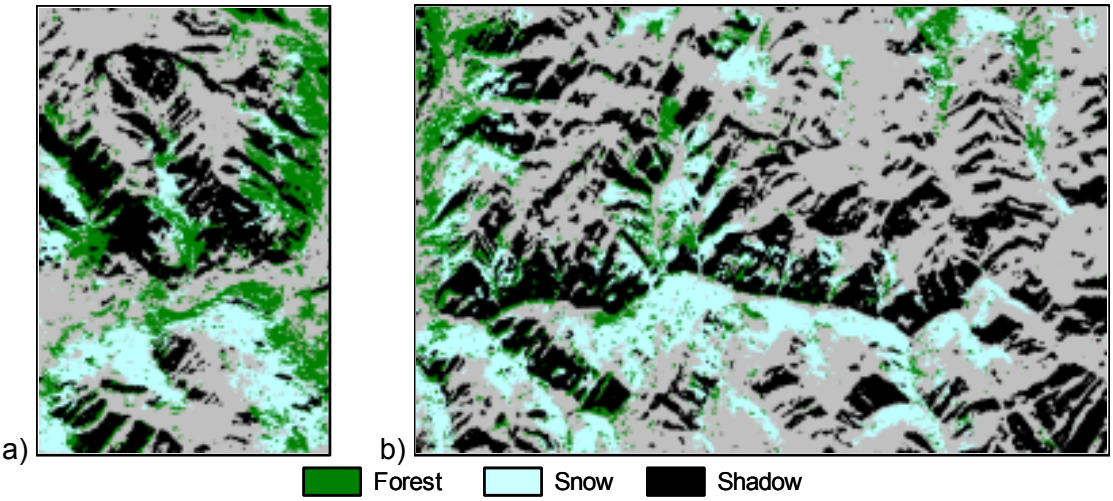

Figure 2: $\Delta \underline{\alpha}$ *images for snow-covered forests over Risoul (a) and Izoard (b), snow-free and unforested areas are in grey*

Snow covered land discrimination

In order to enhance the weak polarimetric contrast between snow-free and snow-covered surface responses, a more adapted method is proposed in the following parts. With a target power response being generally sensitive to polarisation, it is expected that the snow power response intensity can be optimised for specific emitting-receiving polarisation states in order to localise snow-covered surfaces in alpine areas.

OPCE method

The Optimisation of Polarimetric Contrast Enhancement (OPCE) procedure is a well known approach which optimises transmitting and receiving polarisation states to maximize the response of a target with respect to its background (8,9,10). The resulting ρ_{opce} image shows that similar values of polarimetric contrast may be obtained over snow-covered or snow-free (valley or pasture fields) areas (11), similarly to what is reported in (12).

Supervised PCVE procedure: principle

In order to overcome the problems encountered with the OPCE technique, a new method called Polarimetric Contrast Variation Enhancement (PCVE) is introduced. This technique determines emitting and receiving polarisation states that maximise a summer to winter contrast over snow-covered areas while maintaining this contrast to low values over snow-free zones. The PCVE ap-

proach may be decomposed in two steps. First, a supervised procedure determines emitting and receiving polarisation states $(\mathbf{g}_{\max}, \mathbf{h}_{\max})$ that maximise the contrast ratio:

$$[\mathbf{h}_{\max}, \mathbf{g}_{\max}] = Arg \max_{(\mathbf{h},\mathbf{g})} \left(\frac{\rho a}{\rho b} \right) \tag{6}$$

where:

$$\frac{\rho a}{\rho b} = \frac{1}{N_a} \sum_{N_a} \frac{\mathbf{h}^T \mathbf{K_{a\,win}}\, \mathbf{g}}{\mathbf{h}^T \mathbf{K_{a\,sum}}\, \mathbf{g}} \Bigg/ \frac{1}{N_b} \sum_{N_b} \frac{\mathbf{h}^T \mathbf{K_{b\,win}}\, \mathbf{g}}{\mathbf{h}^T \mathbf{K_{b\,sum}}\, \mathbf{g}}$$

The Kennaugh matrices of Eq. (6) are sampled over *a priori* known snow-free and snow-covered areas denoted by the subscripts *a* and *b* respectively. These matrices have to be sampled so as to represent a reasonable range of underlying soil and topography conditions. The PCVE being based on intensity ratios, it is expected to show a reduced sensitivity to the scene topography as mentioned in (13).

The second step consists in applying the optimisation result $(\mathbf{g}_{\max}, \mathbf{h}_{\max})$ to the whole image. A maximal ratio ρ_{pcve} is computed with the specific optimal couple over each cluster of the winter and summer images.

$$\rho \max = \frac{\mathbf{h}_{\mathbf{max}}^T \mathbf{K_{win}}\, \mathbf{g_{max}}}{\mathbf{h}_{\mathbf{max}}^T \mathbf{K_{sum}}\, \mathbf{g_{max}}} \tag{7}$$

A value superior to 1 (0 dB) for ρ_{pcve} indicates a snow-covered surface.

Supervised PCVE procedure: application

The PCVE method is applied to SIR-C SAR data at C-band in summer and winter over the test sites of Risoul and Izoard. Learning areas are selected over the Risoul site to build the summer and winter $\mathbf{K_a}$ and $\mathbf{K_b}$ matrix set used in Eq. (5). Sampling locations may be determined from auxiliary optical information. The optimal couple $(\mathbf{g}_{\max}, \mathbf{h}_{\max})$ is then applied to each cluster of the surface class mask previously determined, in order to obtain a maximal ratio ρ_{pcve} image (11). Figure 3 shows the optimal ratio image resulting from Eq. (6). A comparison of the maps derived from the PCVE procedure with Landsat optical images shows a good estimation of the snow-covered surfaces. One may note the good generalisation properties of the supervised step demonstrated by the results obtained on the Izoard site with maximal polarisation states learned over the Risoul one.

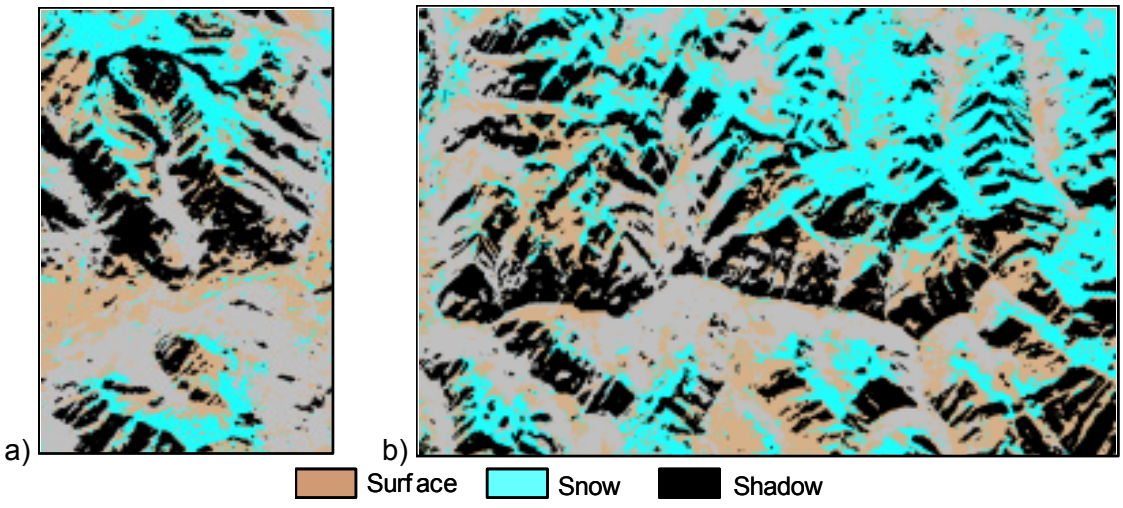

Figure 3: Optimal ratio images for snow covered surfaces over Risoul (a) and Izoard (b) snow free and non-surface areas are represented in grey

RESULTS

Dry snow detection results over surfaces and forested areas are gathered into a single image represented in Figure 4. Test areas are selected in such a way that they are equally distributed over the optical Landsat image, in order to build a reference image. A uniform sampling of *a priori* snow-covered areas is then realised using this reference image and empirical probabilities of detection are estimated. The good detection probability of dry snow is found to equal 81% over Risoul and Izoard.

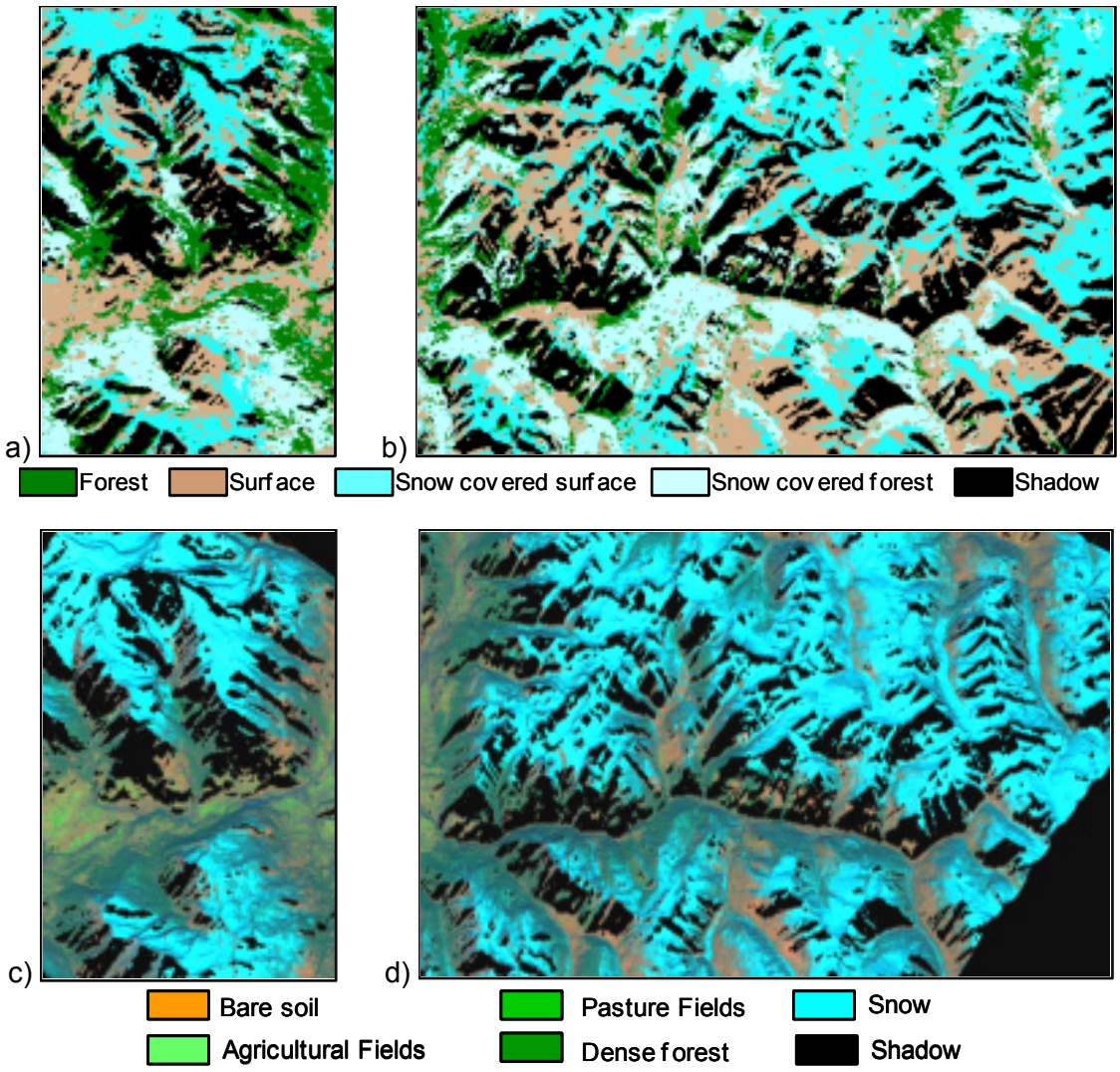

Figure 4: Global snow discrimination result over surfaces and forested areas of Risoul (a) and Izoard (b) and corresponding Landsat optical images (c) and (d)

CONCLUSIONS

The localisation of dry snow using intermediate frequency SAR measurements still remains an active research field, due to the weak influence of dry snow over underlying media scattering properties.

In this paper, we propose a fully polarimetric method to map the dry snow extent in alpine areas using multi-temporal polarimetric SIR-C SAR data with good results. A study of the influence of the underlying medium on a dry snow cover response showed that basic types of environments, like surface or forest, had to be discriminated and processed separately through adapted snow detection procedures. This classification was achieved, at L-band, by gathering an interpretation of polarimetric decomposition results with unsupervised statistical segmentation techniques. An original

PCVE method, based on the maximisation of polarimetric contrast ratios, was proposed to discriminate snow over surfaces. This technique permitted to overcome limitations encountered with classical polarimetric procedures, and its application to seasonal C-band measurements provided an efficient discriminator. Over forested areas, variations of the relevant polarimetric indicator α, computed from seasonal C-band data, were used to discriminate the presence of dry snow. Discrimination results obtained over surfaces and forests were merged to form a global dry snow map. A quantitative estimation of the mapping performance using winter Landsat optical images revealed a good detection probability of 81% for dry snow-covered areas over the Risoul and Izoard sites.

ACKNOWLEDGEMENTS

This study was funded by the CNRS and the French National Space Programme (PNTS-2003, #56). We are also grateful to all those who collected data for snow field measurements (Météo-France, EDF).

REFERENCES

1 Shi J, J Dozier & H Rott, 1993. Modeling and observation of polarimetric SAR response to dry snow. In: Proc. of Int. Geoscience and Remote Sensing Symposium, IGARSS'93. IEEE No. 93CH3294-6, 1042-1045

2 Bernier M & J P Fortin, 1998. The potential of time series of C-band SAR data to monitor dry and shallow snow cover. IEEE Transactions on Geosciences and Remote Sensing, 36(1): 226-241

3 Martini A, L Ferro-Famil & E Pottier, 2004. Snow Extent Discrimination in Alpine Areas from Polarimetric and Multi-Frequency SAR Data. In: EUSAR 2004, Proceedings of the 5th European Conference on Synthetic Aperture Radar (VDE Verlag) 71-75

4 Cloude S & E Pottier, 1995. A review of target decomposition theorems in radar polarimetry. IEEE Transactions on Geosciences and Remote Sensing, 34(2): 498-518

5 Ferro-Famil L, 2000. Télédétection multi-fréquentielle et multi-temporelle d'environnements naturels à partir de données SAR polarimétriques. PhD Dissertation, Université de Nantes, Nantes, France

6 Ferro-Famil L, E Pottier & J S Lee, 2001. Unsupervised classification of multifrequency and fully polarimetric SAR Images based on the H/A/Alpha Wishart classifier. IEEE Transactions on Geosciences and Remote Sensing, 39(11): 2332-2342

7 Cloude S R & E Pottier, 1997. An entropy based classification scheme for land applications of polarimetric SAR. IEEE Transactions on Geosciences and Remote Sensing, 35(1): 68-78

8 Yang J, Y Yamaguchi, W M Boerner & S Lin, 2000. Numerical Methods for Solving the Optimal Problem of Contrast Enhancement. IEEE Transactions on Geosciences and Remote Sensing, 38(2): 965-971

9 Ioannidis G A & D E Hammers, 1979. Optimum antenna polarizations for target discrimination in clutter. IEEE Transactions on Antennas Propagation, AP-27: 357-363

10 Boerner W M, C-L Liu & X Zhang, 1993. Comparison of the optimization procedures for the 2 x 2 Sinclair and the 4 x 4 Mueller matrices in the coherent polarimetry application to radar target versus background clutter discrimination in microwave sensing and imaging. International Journal of Advances in Remote Sensing, 2: 55-82

11 Martini A, L Ferro-Damil & E Pottier, 2004. Multi-frequency polarimetric snow discrimination in Alpine areas. In: Geoscience and Remote Sensing Symposium, 2004. IGARSS '04. Proceedings, 6: 3684-3687

12 Ulaby F W & C Elachi, 1990. Radar Polarimetry for Geoscience Applications (Artech House, Norwood, MA, USA) 595 pp.

13 Floricioiu D, 1997. Polarimetric signatures and classification of alpine terrain by means of SIR-C/ X-SAR. PhD Dissertation (University of Innsbruck, Innsbruck, Austria) 184 pp.